

Dynamics of a suspension of interacting yolk-shell particles

L. E. Sánchez Díaz[†], E. C. Cortes-Morales[‡], X. Li[†], Wei-Ren Chen[†], and M. Medina-Noyola[‡]
[†]*Biology and Soft Matter Division, Oak Ridge National Laboratory, Oak Ridge, Tennessee 37831, USA and*
[‡]*Instituto de Física “Manuel Sandoval Vallarta”, Universidad Autónoma de San Luis Potosí,
Álvaro Obregón 64, 78000 San Luis Potosí, SLP, México*
(Dated: May 24, 2021)

In this work we study the self-diffusion properties of a liquid of hollow spherical particles (shells) bearing a smaller solid sphere in their interior (yolks). We model this system using purely repulsive hard-body interactions between all (shell and yolk) particles, but assume the presence of a background ideal solvent such that all the particles execute free Brownian motion between collisions, characterized by short-time self-diffusion coefficients D_s^0 for the shells and D_y^0 for the yolks. Using a softened version of these interparticle potentials we perform Brownian dynamics simulations to determine the mean squared displacement and intermediate scattering function of the yolk-shell complex. These results can be understood in terms of a set of effective Langevin equations for the N interacting shell particles, pre-averaged over the yolks' degrees of freedom, from which an approximate self-consistent description of the simulated self-diffusion properties can be derived. Here we compare the theoretical and simulated results between them, and with the results for the same system in the absence of yolks. We find that the yolks, which have no effect on the shell-shell static structure, influence the dynamic properties in a predictable manner, fully captured by the theory.

PACS numbers: 64.70.Pf, 61.20.Gy, 47.57.J-

INTRODUCTION

In recent years, there has been a growing interest in designing and manufacturing new materials with nano and microparticles having specifically tailored morphologies, such as core-shell and hollow structures [1–3]. A particularly interesting morphology refers to yolk-shell particles, in which a hollow shell carries a smaller particle in its interior [1, 4]. Nanostructures of this type can be synthesized for application in various fields such as nanoreactors [4], lithium-ion batteries [5], biomedical imaging [5], catalysis [6], and energy storage devices [5]. An essential aspect of the technological use of yolk-shell systems refers to the understanding of their structural and dynamic properties in terms of the yolk-yolk, yolk-shell, and shell-shell direct interaction forces. For example, besides the obvious steric forces that keep a yolk inside its shell, in concentrated samples one may have to consider the interactions between yolk-shell complexes. A basic and elementary question, for example, refers to the effect of the yolk-shell interaction on the Brownian motion of the complex, as exhibited by the difference between the Brownian motion of an empty shell, and of a shell carrying its yolk. A second question refers to the effects of the interactions between yolk-shell complexes on the individual and collective diffusion of interacting yolk-shell complexes.

As a first step to address these questions, in this work we consider a simple model representation of this class of materials, namely, a monodisperse colloidal suspension formed by N rigid spherical shell particles of outer (inner) diameter σ_s (σ_{in}) in a volume V , each of which bears one smaller (“yolk”) rigid particle of diameter σ_y ($< \sigma_{in}$) diffusing in its interior. Here we perform Brownian dy-

namics simulations to describe how the mean squared displacement (MSD) $W(t) = \langle [\Delta \mathbf{R}(t)]^2 \rangle / 6$ and the self-intermediate scattering function (self-ISF) $F_S(k, t) \equiv \langle \exp[i\mathbf{k} \cdot \Delta \mathbf{R}(t)] \rangle$ of tagged yolk-shell particles are influenced by the combined effect of the interaction of the shells with their own yolks and with the other shells, as we vary the concentration $n \equiv N/V$ of yolk-shell particles. We then interpret the results in terms of a model liquid of effective interacting shells, whose Brownian motion is “renormalized” by a time-dependent added friction that results from averaging over the yolks degrees of freedom. This interpretation is developed in the framework of the self-consistent generalized Langevin equation (SCGLE) theory of colloid dynamics, which is adapted here to the context of a suspension of Brownian yolk-shell particles.

As our fundamental starting point, let us consider a model monodisperse yolk-shell colloidal suspension formed by N spherical shell particles in a volume V , each bearing one smaller yolk particle diffusing in its interior. Let us neglect hydrodynamic interactions and denote by $\mathbf{x}_i(t)$ and $\mathbf{v}_i(t)$ the position and velocity of the center of mass of the i th shell ($1 \leq i \leq N$) or yolk ($N+1 \leq i \leq 2N$) particle. Let us denote by M_s and M_y the mass of, respectively, the shell and the yolk particles, and by ζ_s^0 and ζ_y^0 their respective short-time friction coefficients. Then the postulated microscopic dynamics of these $2N$ Brownian particles is described by the following $2N$ Langevin equations,

$$M_i \frac{d\mathbf{v}_i(t)}{dt} = -\zeta_i^0 \mathbf{v}_i(t) + \mathbf{f}_i^0(t) + \mathbf{F}_i(t), \quad (1)$$

with $M_i = M_s$ and $\zeta_i^0 = \zeta_s^0$ for $1 \leq i \leq N$, and $M_i = M_y$ and $\zeta_i^0 = \zeta_y^0$ for $N+1 \leq i \leq 2N$. In these equations,

$\mathbf{f}_i^0(t)$ is a Gaussian white random force of zero mean, and variance given by $\langle \mathbf{f}_i^0(t) \mathbf{f}_j^0(0) \rangle = k_B T \zeta_i^0 2\delta(t) \delta_{ij} \mathbf{I}$ (with \mathbf{I} being the 3×3 unit tensor, T the temperature, and k_B Boltzmann's constant) and $\mathbf{F}_i(t)$ is the force exerted by all the shells and yolks on the i th particle at time t . These forces are assumed to be pairwise additive and determined by the radially symmetric pair potentials $u_{ss}(r)$, $u_{sy}(r) = u_{ys}(r)$, and $u_{yy}(r)$ describing, respectively, the shell-shell, shell-yolk, and yolk-yolk direct interactions. For concreteness, here we shall have in mind a yolk-shell model in which the yolks only interact with their own shells, so that $u_{yy}(r) = 0$. Furthermore, the specific case analyzed below will involve purely repulsive hard-body interactions, defined by the conditions $\exp[-\beta u_{ss}(r)] = H(r - \sigma_s)$ and $\exp[-\beta u_{ys}(r)] = H((\sigma_{in} - \sigma_y)/2 - r)$, where $H(x)$ is Heaviside's step function and $\beta \equiv 1/k_B T$.

Our Brownian dynamics simulations consist essentially of the numerical solution of the overdamped version of these $2N$ stochastic Langevin equations, in which one neglects the inertial terms $M_s [d\mathbf{v}_i(t)/dt]$, according to the algorithm proposed by Ermak and McCammon [7]. We have used this algorithm in the efficient, low-memory version proposed in Ref. [8] to calculate the dynamic properties of the system above. The results will be employed to assess the numerical accuracy of the statistical mechanical description provided by the self-consistent generalized Langevin equation (SCGLE) theory of colloid dynamics [9–14], adapted here to the context of a suspension of Brownian yolk-shell particles. This theory also starts from the same microscopic dynamics represented by the $2N$ Langevin equations in Eqs. (1), but its general strategy is to first average out the degrees of freedom of the yolk particles, which is equivalent to “solving” Eqs. (1) for $N + 1 \leq i \leq 2N$, i.e., for the positions and velocities of the yolk particles, and substituting the solution in Eqs. (1) for $1 \leq i \leq N$. Such procedure, detailed elsewhere [15], yields the following set of N “renormalized” Langevin equations involving the positions and velocities of only the shell particles

$$M_s \frac{d\mathbf{v}_i(t)}{dt} = -\zeta_s^0 \mathbf{v}_i(t) - \int_0^t dt' \Delta\zeta_y(t-t') \mathbf{v}_i(t') + \mathbf{f}_i(t) + \mathbf{F}_i(t) \quad (2)$$

for $i = 1, 2, \dots, N$, where now $\mathbf{F}_i(t)$ only involves shell-shell interactions and the random force $\mathbf{f}_i(t)$ has zero mean and variance given by $\langle \mathbf{f}_i(t) \mathbf{f}_j(0) \rangle = k_B T [\zeta_s^0 2\delta(t) + \Delta\zeta_y(t)] \delta_{ij} \mathbf{I}$. Within a reasonable set of approximations, the time-dependent friction function $\Delta\zeta_y(t)$ can be written as

$$\Delta\zeta_y(t) = \frac{k_B T n_0}{3(2\pi)^3} \int d^3k [k g_{ys}(k)]^2 e^{-k^2 D_y^0 t} F_S(k, t), \quad (3)$$

with $g_{ys}(k)$ being the Fourier transform of $g_{ys}(r) \equiv \exp[-\beta u_{ys}(r)]$ and $n_0 \equiv 1/\int \exp[-\beta u_{ys}(r)] d^3r$.

The second stage in this strategy is to start from this set of N renormalized Langevin equations to derive a

microscopically-based description of the macroscopic dynamic properties of the yolk-shell Brownian liquid. We do this by adequately extending the SCGLE theory of colloid dynamics. Omitting the details of the derivations and approximations, the end result is a set of three coupled approximate equations. The first of these is an approximate expression for the time-dependent friction function $\Delta\zeta_s(t)$ representing the friction on a tracer shell particle due to its direct interactions with the other shells, namely,

$$\Delta\zeta_s(t) = \frac{k_B T}{3(2\pi)^3 n} \int d\mathbf{k} \left[\frac{k[S(k) - 1]}{S(k)} \right]^2 F(k, t) F_S(k, t), \quad (4)$$

where $n \equiv N/V$, $S(k)$ is the (shell-shell) static structure factor, and $F(k, t) \equiv (1/N) \left\langle \sum_{i,j=1}^N e^{i\mathbf{k} \cdot (\mathbf{r}_i(t) - \mathbf{r}_j(0))} \right\rangle$ is the collective intermediate scattering function. The other two equations are approximate expressions for $F(k, t)$ and $F_S(k, t)$, which in Laplace space read

$$F(k, z) = \frac{S(k)}{z + \frac{k^2 S^{-1}(k) D_s^0}{1 + \Delta\zeta_y^*(z) + \lambda(k) \Delta\zeta_s^*(z)}} \quad (5)$$

and

$$F_S(k, z) = \frac{1}{z + \frac{k^2 D_s^0}{1 + \Delta\zeta_y^*(z) + \lambda(k) \Delta\zeta_s^*(z)}}, \quad (6)$$

with $\lambda(k)$ given by [14]

$$\lambda_\alpha(k) = 1/[1 + (k/k_c)^2], \quad (7)$$

and $k_c = 1.305(2\pi/\sigma)$ being an empirically-chosen cutoff wave-vector. This specific choice results from a previous calibration with the properties of hard-sphere systems [16].

We have solved Eqs. (3)-(7) for our yolk-shell model above, for given static structural properties $g_{ys}(k)$ and $S(k)$, with the $S(k)$ provided by the Percus-Yevick [17] approximation with its Verlet-Weis correction [18]. From this solution, all the collective and self-dynamic properties are determined, which we illustrate here with the results for $W(t)$ and $F_S(k, t)$. These properties were also determined in our BD simulations and performed in a conventional fashion [19], except that in practice we followed the method introduced in Refs. [20, 21], which involves a softened version of the potential above to describe the interactions among yolk and shell particles, since the BD algorithm is only rigorously defined for continuous pair potentials. The details of these simulations, as well as the derivation of Eqs. (3)-(7), are provided elsewhere [22]. Let us mention that all the results discussed in this paper correspond to a fixed yolk-shell geometry, in which the thickness ($\sigma_s - \sigma_{in}$) of the shell is 5% of the shell's outer diameter, $\sigma_{in}/\sigma_s = 0.9$, and in which the yolk's diameter is 0.2 in units of σ_s , i.e., $\sigma_y/\sigma_s = 0.2$.

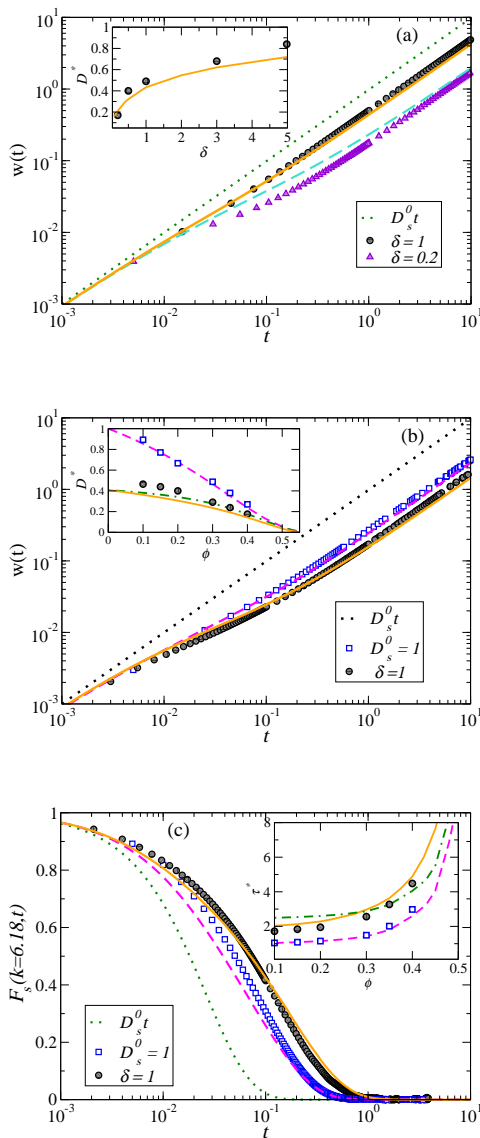


FIG. 1: (a) Mean square displacement $W(t; \phi = 0)$ of non-interacting yolk-shell particles, (b) the MSD $W(t; \phi = 0.4)$, and (c) the self-intermediate scattering function $F_s(k = 6.18, t)$ at volume fraction $\phi = 0.4$. For all figures, shell thickness $(\sigma_s - \sigma_{in})/2 = 0.05$ (or $\sigma_{in} = 0.9$) and yolk diameter $\sigma_y = 0.2$. Recall that we take σ_s as the units of length and σ_s^2/D_s^0 as the time unit. For each figure, circles plot the Brownian dynamics data for the yolk-shell particles, whereas the solid line is the corresponding theoretical prediction of the SCGLE theory with a dynamic asymmetry parameter of $\delta \equiv D_y/D_s^0 = 1$. In figures (a) and (b) the dotted line represents the MSD $W_0(t; \phi = 0) = D_s^0 t$ of a freely diffusing empty shell, and in (c) it represents the self-ISF $F_s^0(k, t; \phi = 0) = \exp(-k^2 D_s^0 t)$ for the same. In (a), the triangles plot the Brownian dynamics data and the dashed line plots the theoretical prediction, both corresponding to $\delta = 0.2$. In the case of (b) and (c), the squares are the simulation data for the empty shell particles, and the dashed line is the corresponding theoretical prediction of the SCGLE theory with short-time diffusion coefficient $D_s^0 = 1$. The inset of (a) shows the long-time self-diffusion D^* as function δ . The insets in figures (b) and (c) are the long-time self-diffusion D^* and $\tau^* (\equiv k^2 D_s^0 \tau_\alpha)$ respectively, both as function ϕ . Symbols and lines for these insets are the same as described in their own main figures. The dot-dashed line in inset (b) is the prediction for D^* using eq. (8), and (c) shows the same prediction for the value of τ^* .

The results reported below will be expressed using σ_s and σ_s^2/D_s^0 as the units of length and time, respectively.

We begin by analyzing the results in Fig. 1 of our Brownian Dynamics simulations for the mean squared displacement $W(t; \phi, \delta)$ of tagged yolk-shell particles, varying the shell volume fraction $\phi \equiv \pi n \sigma_s^3/6$ and the dynamic asymmetry parameter $\delta \equiv D_y/D_s^0$. These results will be compared with the mean squared displacement $W^{(HS)}(t; \phi)$ of the corresponding system of *empty* shells, equivalent in our model to the MSD of a Brownian hard-sphere liquid at volume fraction ϕ [20, 21]. Fig. 1(a) and 1(b) contain, respectively, the results for $W(t; \phi, \delta)$ at $\phi = 0$ (freely-diffusing yolk-shells) and $\phi = 0.4$ (strongly-interacting yolk-shells). Fig. 1(a) is intended to illustrate two effects in a simple manner. The first is the effect of yolk-shell interactions, which is illustrated by the comparison of the circles, representing the MSD $W(t; \phi = 0, \delta = 1)$ of freely diffusing yolk-shell particles, and the dotted line, representing the MSD $W_0(t) \equiv D_s^0 t$ of freely diffusing *empty* shells. The deviation of the simulation data from $W_0(t)$ is a measure of the additional friction effects upon the displacement of the yolk-shell complex due to the yolk-shell interaction. The solid line that lies near the circles represents the prediction of our SCGLE theory. The first conclusion that we can draw from this comparison is that the SCGLE-predicted deviation of $W(t; \phi = 0, \delta = 1)$ from $W_0(t)$, coincides very satisfactorily with the deviation observed in the BD data.

The second effect illustrated by Fig. 1(a) involves the dynamic asymmetry parameter. The next conclusion to draw from the results in this figure is that the deviation of $W(t; \phi = 0, \delta)$ from $W_0(t)$ increases when the dynamic contrast parameter δ decreases. This is illustrated by the comparison of the BD simulations corresponding to $\delta = 0.2$ (triangles) with the BD data corresponding to $\delta = 1.0$ (circles). This means, for example, that if the interior of the shell becomes more viscous, so that the ratio δ decreases, then also the overall diffusivity of the yolk-shell particle will decrease. As evidenced by the solid and dashed lines in Fig. 1(a), this trend is also predicted by the SCGLE theory and shows good quantitative agreement with the simulation data. In fact, our theory predicts, and the simulations corroborate, that this trend is reversed when one considers the opposite limit, in which δ is now larger than 1. This trend is best illustrated in the inset of Fig. 1(a), which exhibits the measured (circles) and predicted (solid line) dependence on δ of the scaled long-time self-diffusion coefficient $D^*(\phi, \delta) \equiv D_L/D_s^0$, obtained as $D^*(\phi, \delta) = \lim_{t \rightarrow \infty} W(t; \phi, \delta)/D_s^0 t$. There we can see that the reduction of the mobility $D^*(\phi = 0, \delta)$ from its unit value $D_{HS}^*(\phi = 0) = 1$, in the absence of yolks, may be considerable. For example, for $\delta = 0.2$ we have that $D^*(\phi = 0, \delta) \approx 0.17$. As a reference, a reduction in $D_{HS}^*(\phi)$ of a similar magnitude can also be produced as a result of pure shell-shell interactions, but only at shell volume fractions above 40%, as gathered

from the results of the inset in Fig. 1(b), which discusses the effects of shell-shell interactions.

Let us now study the effects of shell-shell interactions, suppressed in the previous discussion, by analyzing the results of our simulations in Fig. 1(b), in which we now fix the dynamic asymmetry parameter at the value $\delta = 1$. The circles in this figure represent the BD results for the MSD $W(t; \phi = 0.4, \delta)$ of yolk-shell particles at a volume fraction $\phi = 0.4$. These results are to be compared with the squares, which correspond to the BD results for the MSD $W^{(HS)}(t; \phi = 0.4)$ of a liquid of empty shells (or solid hard-spheres) at the same volume fraction and same short-time self-diffusion coefficient D_s^0 . The MSD $W_0(t) = D_s^0 t$ of freely-diffusing empty shells is also plotted for reference as a dotted line. We observe that the deviation of $W(t; \phi = 0.4, \delta)$ from $W^{(HS)}(t; \phi = 0.4)$ remains rather similar to the corresponding deviation observed at $\phi = 0$ in Fig. 1(a) (where $W^{(HS)}(t; \phi = 0) = D_s^0 t$), but now both $W(t; \phi = 0.4, \delta)$ and $W^{(HS)}(t; \phi = 0.4)$ deviate dramatically from this free-diffusion limit. This means that for this concentration, the mutual friction effects due to shell-shell interactions overwhelm the “internal” friction effects caused by yolk-shell interactions.

From the long-time BD data for $W(t; \phi = 0.4, \delta)$ and $W^{(HS)}(t; \phi = 0.4)$ in Fig. 1(b), we can extract the value of $D^*(\phi, \delta)$ and $D_{HS}^*(\phi)$, which represent the mobility of a tracer yolk-shell particle and of an empty shell, respectively. In the inset of Fig. 1(b), we plot the values of $D^*(\phi, \delta)$ and $D_{HS}^*(\phi)$ (circles and squares, respectively) determined from the corresponding BD results at a few volume fractions. This inset thus summarizes the main trends illustrated by the results in Figs 1.a and 1.b, by evidencing that at low volume fractions the difference between the mobility of a yolk-shell complex and the mobility of an empty shell, is determined only by the yolk-shell friction, whereas at higher concentrations it is dominated by the shell-shell interactions. The solid lines in Fig. 1(b) represent again the predictions of the SCGLE theory for the properties of the yolk-shell system, whereas the dashed lines are the corresponding predictions for the empty-shell (or hard-sphere) suspension. Once again, the agreement with the simulation results is also quite reasonable for a theory with no adjustable parameters.

Beyond this quantitative observation, however, the theoretical description provides additional insights on the interpretation of the qualitative trends exhibited by the simulation data of the long-time self-diffusion coefficients $D^*(\phi, \delta)$ and $D_{HS}^*(\phi)$. For example, it is not difficult to demonstrate that if the shell-shell mutual friction $\int_0^\infty dt \Delta\zeta_s^*(t; \phi, \delta)$ does not depend strongly on the presence or absence of the yolk (which one expects to be the case at high concentrations), then an approximate relationship between $D^*(\phi, \delta)$ and $D_{HS}^*(\phi)$ can be derived,

namely,

$$D^*(\phi, \delta) = \frac{D_0^*(\delta) \times D_{HS}^*(\phi)}{D_{HS}^*(\phi) + D_0^*(\delta)[1 - D_{HS}^*(\phi)]}. \quad (8)$$

where $D_0^*(\delta) \equiv D^*(\phi = 0, \delta) = [1 + \Delta\zeta_y^*(\delta)]^{-1}$, with $\Delta\zeta_y^*(\delta) \equiv \int_0^\infty dt \Delta\zeta_y^*(t; \phi = 0, \delta)$. This expression interpolates $D^*(\phi, \delta)$ between its exact low and high concentration limits $D_0^*(\delta)$ and $D_{HS}^*(\phi)$, and the dot-dashed line in the inset of Fig. 1(b) is the result of using this approximate expression.

The BD simulations and the SCGLE theory provide other relevant collective and self diffusion dynamic properties, such as the intermediate scattering functions, specially amenable to determination by dynamic light scattering techniques and adequate index-matching methods. To close this illustrative presentation, let us discuss the BD results in Fig. 3.c for the self-ISF $F_S(k = 6.18, t; \phi = 0.4, \delta = 1)$ (circles), which we compare with the self-ISF $F_S^{HS}(k = 6.18, t; \phi = 0.4)$ of a liquid of empty-shells at the same volume fraction (squares). For reference, we also plot as a dotted line the self-ISF $F_S^0(k, t) \equiv F_S^{HS}(k, t; \phi = 0) = \exp(-k^2 D_s^0 t)$ of freely-diffusing empty shells. Here too, the solid and dashed lines correspond to the solution of Eqs. (3)-(7) with and without the shell friction term $\Delta\zeta_y^*(t)$, and comparison again indicates very reasonable agreement with the simulation data.

In this case, the difference between the yolk-shell and empty-shell results can also be expressed more economically in terms of the corresponding α -relaxation times τ_α , defined by the condition $F_S(k, \tau_\alpha) = 1/e$ and scaled as $\tau^* \equiv k^2 D_s^0 \tau_\alpha$. The inset of Fig. 1(c) exhibits the theoretical (solid line) and simulated (circles) results for the yolk-shell $\tau^*(k; \phi, \delta)$ evaluated at $k = 6.18$ for $\delta = 1$ as a function of ϕ . These results may be compared with the theoretical (dashed line) and simulated (squares) results for $\tau_{HS}^*(k = 6.18; \phi = 0.4)$, corresponding to the empty-shell suspension, with similar conclusions as in Fig. 1(b). In analogy with the relationship in Eq. (8), from the SCGLE equations one can also derive an approximate relationship between $\tau^*(k; \phi, \delta)$ and $\tau_{HS}^*(k; \phi)$, namely, $\tau^*(k; \phi, \delta) \approx \tau_{HS}^*(k; \phi) + \Delta\zeta_y^*(\delta)$. This prediction of the value of $\tau^*(k; \phi, \delta)$ has a rather modest quantitative accuracy, as indicated by the dot-dashed line in the inset. Still, it contributes to a simple and correct qualitative understanding of the main features of the properties of the yolk-shell system being studied.

In summary, in this work we have carried out BD simulations and have proposed a statistical mechanical approach for describing the dynamic properties of a complex system, namely, a concentrated suspension of yolk-shell particles. Here we have discussed the simplest illustrative model representation, in which each shell carries only a single yolk, and in which the yolk-shell and shell-shell forces are model as purely repulsive, hard-

body interactions. This implied an additional simplification, namely, the absence of yolk-yolk direct interactions. These simplifications allowed us to reach a reasonable understanding of the differences between a yolk-shell system and a suspension of empty shell, and of the main trends observed upon the variation of relevant parameters, such as the short-time dynamic asymmetry parameter δ or the shell volume fraction ϕ . The message, however, is that the theoretical approach presented here can be extended to consider other, more complex conditions, such as including more than one yolks per shell and studying the effects of yolk-shell and shell-shell interactions beyond the purely repulsive, hard-core-like interactions considered here.

ACKNOWLEDGMENTS

This work was supported by the U.S. Department of Energy, Office of Basic Energy Sciences, Materials Sciences and Engineering Division. This Research at the SNS at Oak Ridge National Laboratory was sponsored by the Scientific User Facilities Division, Office of Basic Energy Sciences, U.S. Department of Energy. This work was also supported by the Consejo Nacional de Ciencia y Tecnología (CONACYT, Mexico), through Grants No. 132540 and No. 182132.

- [2] S. H. Joo, J. Y. Park, C. K. Tsung, Y. Yamada, P. D. Yang, G. A. Somorjai, *Nat. Mater.* 2009, **8**, 126.
- [3] Y. D. Yin, R. M. Rioux, C. K. Erdonmez, S. Hughes, G. A. Somorjai, A. P. Alivisatos, *Science* 2004, **304**, 711.
- [4] K. Kamata, Y. Lu, Y. N. Xia, *J. Am. Chem. Soc.* 2003, **125**, 2384.
- [5] J. Liu, H. Xia, D. F. Xue, L. Lu, *J. Am. Chem. Soc.* 2009, **131**, 12086.
- [6] H. X. Li, Z. F. Bian, J. Zhu, Y. N. Huo, H. X. Li, Y. F. Lu, *J. Am. Chem. Soc.* 2007, **129**, 8406.
- [7] D. L. Ermak and J. A. McCammon. *J. Chem. Phys.* **69**, 1352 (1978).
- [8] D. Dubbeldam, D. C. Ford, D. E. Ellis, and R. Q. Snurr, *Mol. Sim.* **35**, 1084 (2009).
- [9] L. Yeomans-Reyna and M. Medina-Noyola, *Phys. Rev. E* **62**, 3382 (2000).
- [10] L. Yeomans-Reyna and M. Medina-Noyola, *Phys. Rev. E* **64**, 066114 (2001).
- [11] L. Yeomans-Reyna, H. Acuña-Campa, F. Guevara-Rodríguez, and M. Medina-Noyola, *Phys. Rev. E* **67**, 021108 (2003).
- [12] P.E. Ramírez-González *et al.*, *Rev. Mex. Física* **53**, 327 (2007).
- [13] L. Yeomans-Reyna, M. Chavez-Rojo, P.E. Ramírez-González, R. Juárez-Maldonado, M. Chavez-Paez and M. Medina-Noyola *Phys. Rev. E* **76**, 041504 (2007).
- [14] R. Juárez-Maldonado, M. Chavez-Rojo, P.E. Ramírez-González, L. Yeomans-Reyna and M. Medina-Noyola, *Phys. Rev. E* **76**, 062502 (2007).
- [15] M. Medina-Noyola, *Faraday Discuss. Chem. Soc.* **83**, 21 (1987).
- [16] L. López-Flores, L. L. Yeomans-Reyna and M. Medina-Noyola, *J. Phys.: Condens. Matter* **24**, 375107 (2012).
- [17] J. K. Percus and G. J. Yevick, *Phys. Rev.* **110**, 1 (1957).
- [18] L. Verlet and J.-J. Weis, *Phys. Rev. A* **5** 939 (1972).
- [19] Allen, M. P.; Tildesley, D. J. *Computer Simulation of Liquids*. Oxford University Press: Oxford, 1989.
- [20] F. de J. Guevara-Rodríguez and M. Medina-Noyola, *Phys. Rev. E* **68**, 011405 (2003).
- [21] L. Lopez-Flores, H. Ruiz-Estrada, M. Chávez-Páez and M. Medina-Noyola, *Phys. Rev. E* **88**, 042301 (2013)
- [22] L. E. Sánchez-Díaz, E. C. Cortés-Morales, X. Li, W.-R. Chen, and M. Medina-Noyola, manuscript in preparation (2014).

[1] X.W. Lou, L. A. Archer, Z. Yang, *Adv. Mater.* 2008, **20**, 3987.